MDPI

Article

Absolute Measurement of the Refractive Index of Water by a Mode-Locked Laser at 518 nm

Zhaopeng Meng [1], Xiaoyu Zhai [1,2], Jianguo Wei [1], Zhiyang Wang [3] and Hanzhong Wu [3,*]

[1]   School of Computer Software, Tianjin University, Tianjin 300072, China; mengzp@tju.edu.cn (Z.M.); 1013202057@tju.edu.cn (X.Z.); jianguo@tju.edu.cn (J.W.)
[2]   National Ocean Technology Center, Tianjin 300112, China
[3]   School of Marine Science and Technology, Tianjin University, Tianjin 300072, China; wzy_sxn@tju.edu.cn
[*]   Correspondence: wuhz@tju.edu.cn; Tel.: +86-188-2228-8952

check for updates

Abstract: In this paper, we demonstrate a method using a frequency comb, which can precisely measure the refractive index of water. We have developed a simple system, in which a Michelson interferometer is placed into a quartz-glass container with a low expansion coefficient, and for which compensation of the thermal expansion of the water container is not required. By scanning a mirror on a moving stage, a pair of cross-correlation patterns can be generated. We can obtain the length information via these cross-correlation patterns, with or without water in the container. The refractive index of water can be measured by the resulting lengths. Long-term experimental results show that our method can measure the refractive index of water with a high degree of accuracy—measurement uncertainty at 10^{-5} level has been achieved, compared with the values calculated by the empirical formula.

1. Introduction

During the past decades, marine technology has attracted great attention both as a field of research, and for economical reasons [1]. The resources hidden underwater, such as coal, oil, and natural gas, are receiving increasing interest because of depleting resources on land. Scientists all over the world have developed a wealth of marine instruments, so as to make sailing, as well as resource exploration, convenient and efficient. The acoustic method is the most-widely used technique, owing to a lower attenuation when travelling underwater; however, due to the multipath effect, considerable noise could exist in the signal returns [2–4], resulting in a very complicated data process. In addition, the measurement resolution of the acoustic wave is strongly limited by beam size and divergence. The electro-magnetic wave (~GHz) can be exploited in short distance measurements underwater (tens of meters), based on phase measurement and power attenuation [5,6]. In the case of the phase measurement, accuracy and precision cannot be very high on account of the larger electro-magnetic wavelength. In terms of power attenuation, power-based measurements are negatively affected by extreme environments underwater. In short-path underwater measurements, optical waves, with a transmission window of between 480 nm and 540 nm, are an ideal candidate [7–9]. With excellent laser alignment and inherent high power, the underwater optical technique has shown itself to be highly effective in marine applications [10]. Different from acoustic and electro-magnetic waves, one basic issue associated with the optical method is the correction of the refractive index of water [11].

Measurement of the refractive index of water is of fundamental importance in the application of optical underwater techniques, and various methods have been proposed to address the issue. Analogous with measurements of the refractive index of air, indirectly, the refractive index of water

can be corrected based on a knowledge of the wavelength, temperature, and density of the water, by using an empirical formula [12,13]. Directly, the refractive index of water can be measured using the methods of refraction and interferometrics. Classical schemes mostly rely on Snell's law, e.g., Abbe refractometer [14], Pulfrich refractometer (based on the measurement of the deflection angle of the incident ray on a V-shaped prism [15]), and numerous other variants [16,17]. For these methods, knowledge of the refractive index of the prism is required, as well as the precise determination of the corresponding angles. In general, the measured angles can be determined by autocollimators; however, the resulting system is very complicated, and often involves moveable elements. Measurement uncertainty is at 10^{-4} level. In contrast to refraction methods, the interferometric technique, based on fringe counting, can provide better resolution and lower measurement uncertainty (better than 10^{-5}). Traditionally, a water container (sample cell) is placed in the measurement path of the interferometer [18,19], a Michelson interferometer or Mach-Zehnder interferometer. The refractive index of water can be determined by measuring the optical path difference between the reference and measurement beam, with or without water in the container. Consequently, the geometrical length of the container is required. In this case, the thermal expansion of the water container can make considerably increase measurement uncertainty. To overcome this problem, scientists have proposed many solutions, e.g., the auto-compensating interferometer [20], and the multi-step interferometer [21], etc. B. Richerzhagen presented a configuration of a Michelson interferometer without compensation, where the measurement mirror is fixed in the water [22]. The measurement mirror should be well thermally isolated from the water container, and should be fixed on a moveable stage, to yield an absolute measurement of the refractive index. In addition, dispersive interferometry with a low coherence source [23], and the technique of fiber sensors [24] have also been reported.

Frequency combs have achieved huge success in many applications since their invention [25]. Benefitting from extremely high accuracy and precision of the frequency elements, frequency combs have advanced a wealth of fields, including precision spectroscopy [26], time/frequency transfer [27], and length metrology [28], etc. Length is a fundamental quantity in science and technology. During the past decade, frequency combs have revolutionized techniques of absolute distance measurement, as well as measurements of the quantity related to length, such as thickness [29], vibration/speed [30], surface profiling [31], and refractive index [32], etc. We focus on the measurement of refractive indices in this paper. To date, the measurement of the refractive index of air using a frequency comb has already achieved a 10^{-9} uncertainty [33], far surpassing those obtained using empirical formulas. Thickness and refractive index measurements of solids (glass, wafer) using frequency comb have also been in development for more than a decade [34–36], and various methods have been investigated in great depth. However, there are few reports about measurements of the refractive index of liquids using frequency comb.

In this study, we carried out absolute measurements of the refractive index of water using a frequency comb at 518 nm. We develop an interferometric system, where both the measurement and reference mirrors of the Michelson interferometer are under water in a quartz-glass container. Consequently, the expansion compensation of the water container is not required. Cross-correlation patterns can be obtained with a scanning stage, which can be processed to determine the corresponding lengths. The refractive index of water can be measured via the obtained lengths. Experimental results showed an agreement at 10^{-5} level, compared with the empirical formula [13].

2. Materials and Methods

The experimental setup is shown in Figure 1. The frequency comb (Menlosystem FC1000 (Menlosystem, Martinsried, Germany), 100 MHz repetition frequency, 500 mW maximum output power, 518 nm center wavelength) emits a pulsed laser, which is split at a beam splitter. One part is directed into the Michelson interferometer, which can introduce a measured length L. Please note that the entire Michelson interferometer is placed in the water container, which means that the reference path and the measurement path are thermally expanded at the same time. In addition, the thermal

expansion coefficient of quartz glass is relatively lower. Therefore, the system can automatically compensate for the thermal expansion of the water container. The other part is scanned by using a moving stage (PI M521, PI, Karlsruhe, Germany), 200 mm travel range), and is then combined with the output of the Michelson interferometer at a beam splitter. A photo-detector (PD1, Thorlabs APD430A, Thorlabs, NJ, USA) is used to detect the combined beam, and an oscilloscope (LeCroy 640Zi, LeCroy, NYC, USA) is used to measure and store the cross-correlation patterns. To obtain the precise position of the scanning mirror (MS), a fringe counting interferometer based on a cw laser (Thorlabs HRS015B, Thorlabs, NJ, USA), 632.991 nm, 2 MHz frequency stability) is used as the distance meter. The temperature and the density of water are measured by Valeport Mini SVP in real time, which can be used to calculate the refractive index of water with the empirical formula (i.e., Harvey formula) [13]. Please note that the Harvey formula is used in the case of pure water. In our experiments, we used the tap water, which is sufficiently clean for the Harvey formula to be applicable.
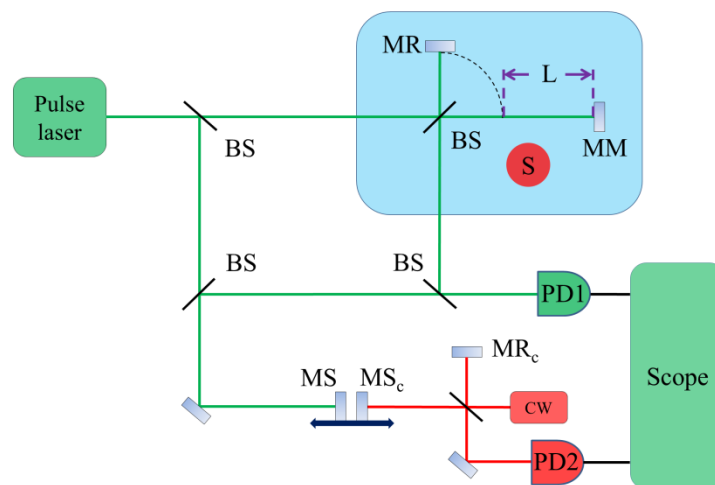

Figure 1. Experimental setup. BS: beam splitter; MR: reference mirror; MM: measurement mirror; S: sensors; PD: photodetector; MS: scanning mirror; MR_c: reference mirror of the cw interferometer; MS_c: scanning mirror of the cw interferometer; cw: continuous wave laser.

We measure the refractive index of water with two steps. First, the water container is not filled with water. We can obtain a length value L_a in air, and $L_a = n_a L$. n_a is the group refractive index of air, which can be corrected by using empirical formulae, and L is the geometrical length difference between the reference and measurement beams of the Michelson interferometer. Second, the water container is full with water. Considering the group refractive index of water, we can obtain a length value L_{gw}, i.e., $n_{gw} L$, where n_{gw} is the group refractive index of water. In the case of phase refractive index at a certain wavelength, the corresponding length value L_p can be expressed as $n_p L$, where n_p is the corresponding phase refractive index of water. Consequently, the group refractive index of water n_{gw} can be calculated as:

$$n_{gw} = \frac{L_{gw}}{L} = \frac{L_{gw}}{L_a / n_a} \tag{1}$$

For a certain wavelength, the phase refractive index of water can be indicated as:

$$n_p = \frac{L_p}{L} = \frac{L_p}{L_a / n_a} \tag{2}$$

After we obtain the values of L_{gw}, L_p, L_a and n_a, the group and phase refractive indices of water can be measured.

3. Results

The source spectrum is shown in Figure 2, with a center wavelength of approximately 518 nm and a spectral width of around 4 nm. The environmental parameters are: 19.2 °C temperature, 1032.5 hPa pressure, and 35% humidity. The group refractive index of air n_a can be calculated as 1.00029157 by Ciddor formula [37].
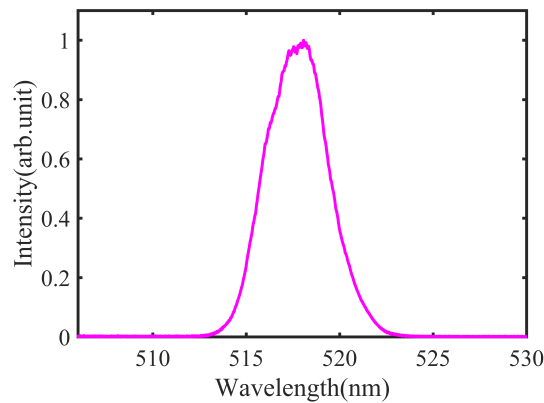
Figure 2. The source spectrum.

3.1. Measurement of Group Refractive Index of Water

In this section, we describe the measurement of the group refractive index of water. The speed of the moving stage is set to 50 mm/s, i.e., travel time for a single stroke is 4 s. First, the water container is not filled with water. We can obtain a pair of cross-correlation patterns, shown in Figure 3a, which correspond to the reference and measurement mirrors respectively. Figure 3b shows a detailed observation of the cross-correlation pattern; in it, we see that the pulse width is about 100 μm (333 fs).
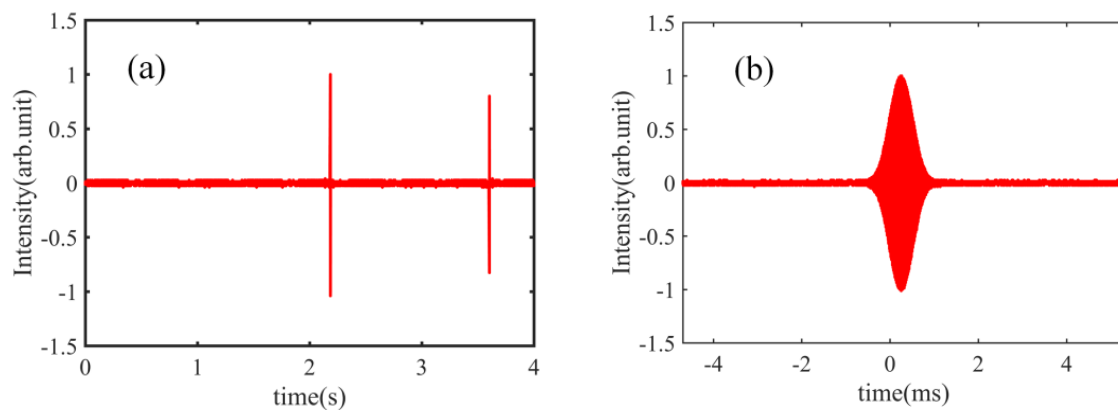
Figure 3. (**a**) Cross-correlation patterns corresponding to the reference mirror and the measurement mirror, without water in the container; (**b**) detailed observation of the cross-correlation pattern, without water in the container.

Performing a Hilbert transform of the cross-correlation patterns in Figure 3a, we can obtain the results shown in Figure 4, where the inset is the curve expansion. Based on the peak positions, the length L_a can be measured, using a fringe counting interferometer, at 70.783 mm. Therefore, length L can be calculated as 70.783 mm/1.00029157, i.e., 70.762 mm.

Second, the container is full with water. The obtained cross-correlation patterns are indicated in Figure 5a. Figure 5b is the expansion of a single cross-correlation pattern in the time axis. We find that, the cross-correlation pattern is obviously broadened to about 350 μm (1.2 ps). This broadening

is due to water dispersion. The length L_{gw} can be measured by the same process as that of Figure 4, and is 96.676 mm. Based on Equation (1), the group refractive index of water can be thus calculated as: 96.676/70.762 = 1.36621. The water conditions were: 14.4 °C temperature and 999.2 kg/m^3 density, and based on the empirical formula, the group refractive index of water can be calculated to be 1.36622. Finally, we find a difference of 1×10^{-5} between our result and that obtained using the empirical formula. Please note that the empirical formula in this work refers to Reference [13].
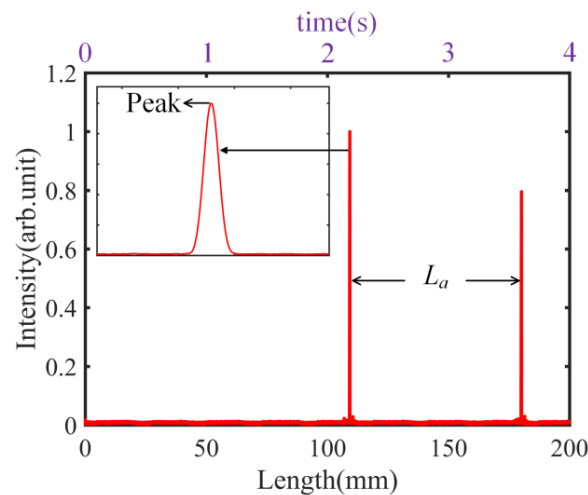

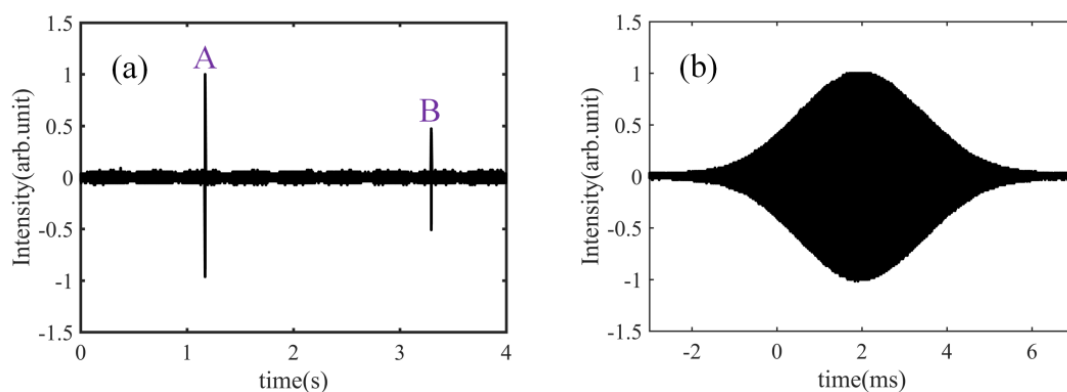**Figure 4.** Results of Hilbert transform.

Figure 5. (**a**) Cross-correlation patterns corresponding to the reference mirror and the measurement mirror, with water in the container; (**b**) detailed observation of the cross-correlation pattern, with water in the container.

We performed a measurement over a 5-h period; the results are shown in Figure 6. In Figure 6a, the red solid line indicates the results obtained by our method, and the black dashed line represents results obtained using the empirical formula. Please note that, for convenience of display, both results are shifted by −1.36622. We observed that the group refractive index of water changed by up to around 3×10^{-4} in a 5-h period. Figure 6b shows the difference between the results obtained using the empirical formula and our method. In long-term experiments, we observed the difference to be be well below 2×10^{-5}.
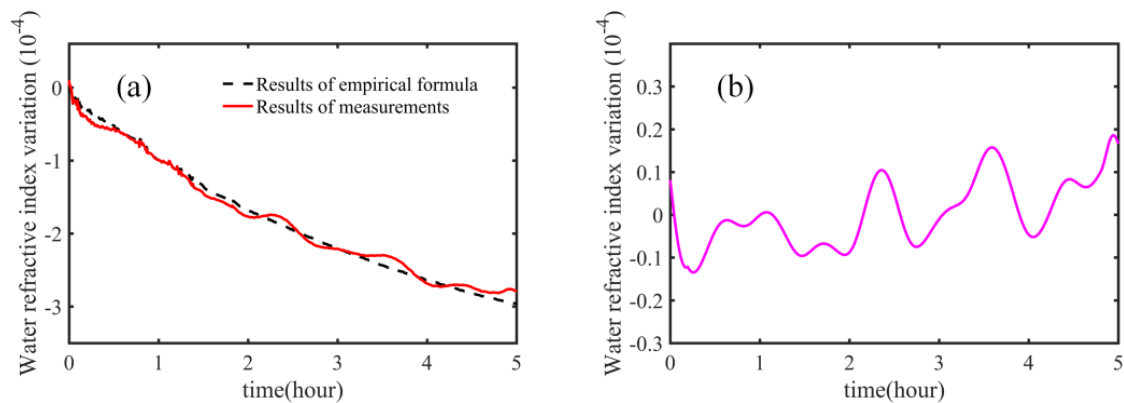
Figure 6. Long time measurements of the group refractive index of water. (**a**) Results obtained using the empirical formula and our measurements; red solid line: result of our method; black dashed line: result of the empirical formula; (**b**) difference between the results of empirical formula and our measurements.

3.2. Measurement of Phase Refractive Index of Water

In this section, we measure the phase refractive index of water at a particular wavelength. Different from the Section 3.1, here we used a Fourier transform to determine the distance for each wavelength. In fact, as a classical method of data processing, Fourier transforms can also be used in Section 3.1. In that case, the length can be measured through the slope of the unwrapped phase, and the results are nearly the same.

Assuming that the phase of the wavelength λ is φ_0 for the reference mirror, and φ_1 for the measurement mirror, the length L_p can be calculated as $(\varphi_1 - \varphi_0)/(2\pi) \times \lambda$ for the wavelength λ [38,39]. Please note that φ_1 and φ_0 are the unwrapped phases. The data process of the Fourier transform is shown in Figure 7. The first cross-correlation pattern, (A) in Figure 5, is picked up, and zero padding is needed. To enhance process efficiency and save memory, we subsample the raw data, which is a mature technique widely used in the signal processing [40,41]; the resulting curve is shown in Figure 7a. Please note that the subsampling coefficient N_0/N_1 should be defined carefully; it must meet the condition that the frequency spectrum of the Fourier transform be completely located within a range from 0 to $f_s/2$ (without spectrum leakage), analogous to the demonstration mentioned in Reference [42]. N_0 is the sample number of the raw data (3×10^6 in our experiments), N_1 is the sample number after subsampling (544 in our experiments), and f_s is the sampling rate. Figure 7b shows the frequency spectrum, and we find that no spectrum leakage exists. Figure 7c,d shows the wrapped phase and unwrapped phase respectively. The data process of the second cross-correlation pattern (B in Figure 5) is the same as that shown in Figure 7. After the phases are obtained, L_p can be determined, and the phase refractive index can be measured based on Equation (2).
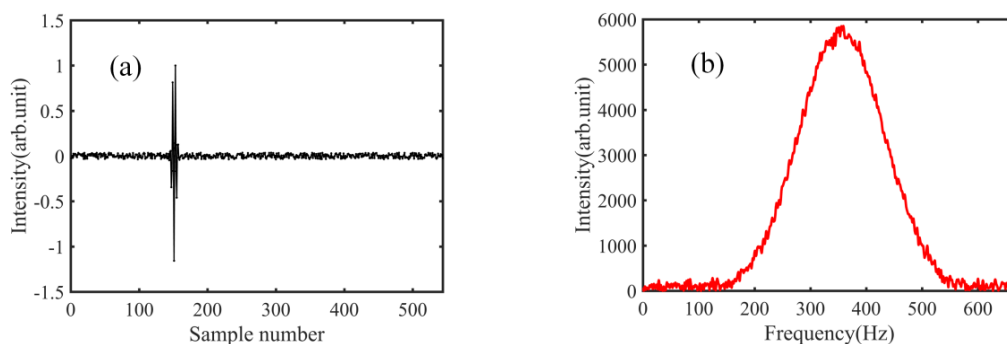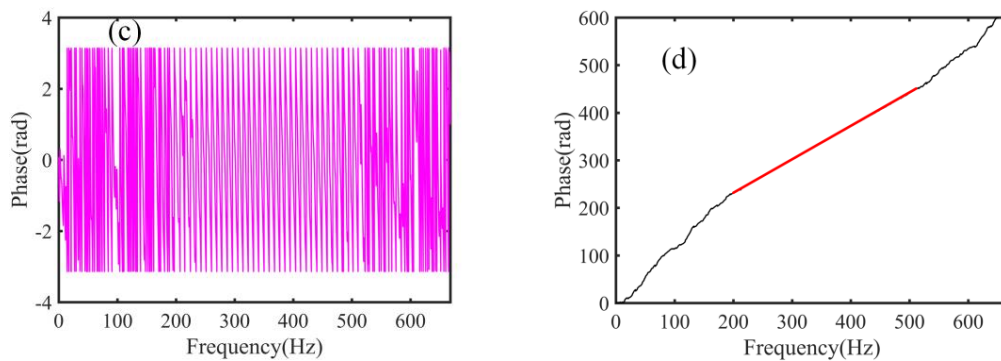

Figure 7. *Cont.*

Figure 7. Fourier transform data process. (**a**) Data after the sub sampling; (**b**) frequency spectrum of Fourier transform; (**c**) wrapped phase of Fourier transform; (**d**) unwrapped phase of Fourier transform.

With water conditions of 14.4 °C and 999.2 kg/m^3, the experimental results of phase refractive index measurements in the spectral range from 515 nm to 521 nm are shown in Figure 8. The pink dashed line indicates the results obtained using our method, and the green solid line shows the those from the empirical formula. In the range from 515 nm to 521 nm, the difference between our method and the empirical formula can be less than 1×10^{-5}. We also find that water dispersion is very significant when green light transmits in water (~2.5×10^{-4} in the 6-nm spectral range), and that the pulse can be strongly broadened.
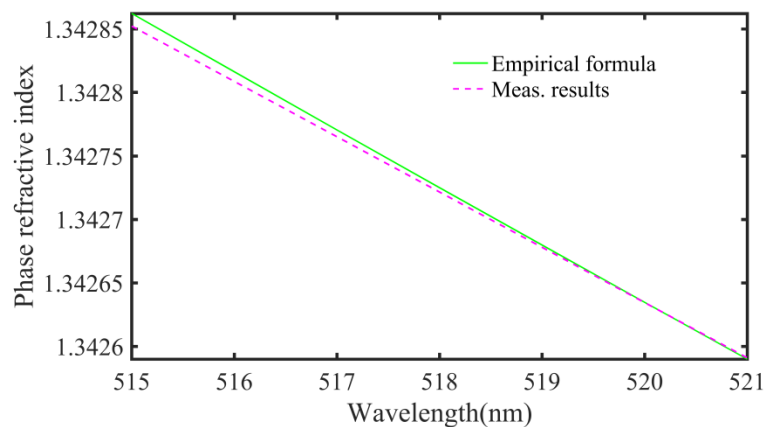

Figure 8. Results of the phase refractive index measurement; pink dashed line: result of our method; green solid line: result of the empirical formula.

We carried out 5-h experiments; the experimental results for 518 nm wavelength (vacuum wavelength) are shown in Figure 9. In Figure 9a, the red solid line indicates the results obtained using our method, and the black dashed line represents those results obtained using the empirical formula. Please note that for convenience of display, both the results are shifted by −1.34272. We found that the results obtained using our method and those from the empirical formula changed under the same law, and the phase refractive index of water at 518 nm varied by up to about 2.5×10^{-4} in a 5-h period. Figure 9b shows the difference between the results obtained using the empirical formula and our method. In long-term experiments, we found measurement uncertainty to be well below 1.2×10^{-5}.
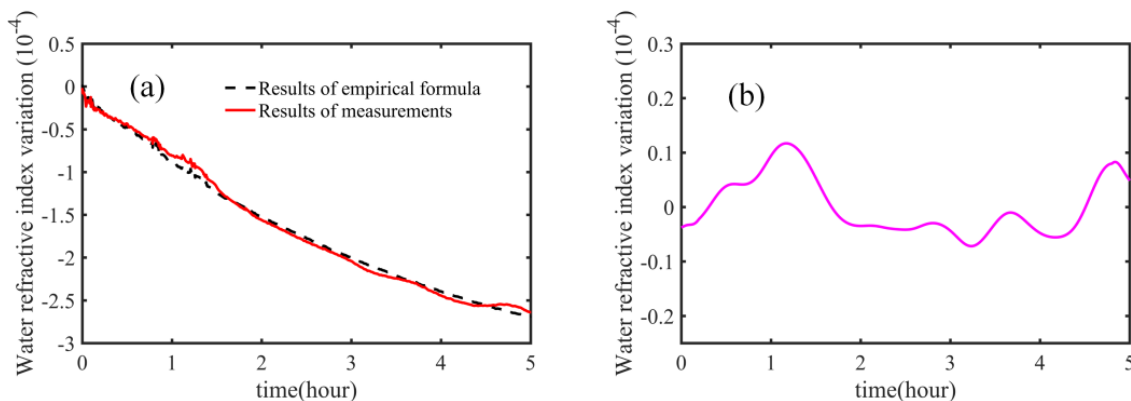
Figure 9. Time measurements of the phase refractive index of water at 518 nm. (**a**) Results of empirical formula and our measurements; red solid line: result of our method; black dashed line: result of the empirical formula; (**b**) difference between the results of empirical formula and our measurements.

4. Uncertainty evaluation

Based on Equation (1), the measurement uncertainty of n_{gw} is related to L_{gw}, L_a and n_a, and can be calculated as:

$$u_{n_{gw}}{}^2 = \left(\frac{L_{gw}}{L_a} u_{n_a} \right)^2 + \left(\frac{n_a}{L_a} u_{L_{gw}} \right)^2 + \left(\frac{n_{gw}}{L_a} u_{L_a} \right)^2 \tag{3}$$

The first term of Equation (3) is related to the refractive index of air n_a based on the Ciddor formula. This part is related to the uncertainty of the Ciddor formula itself, the uncertainty of the sensor network, and the stability of the environment. Considering that the total optical path is relatively short, the inhomogeneity of the environment can be neglected. The average value of L_{gw} is 96.664 mm in 5-h experiments, and L_a equals to 70.783 mm. This part, dependent upon n_a, can thus be evaluated to 1.4×10^{-8}, which is negligible. The second term of Equation (3) is related to the uncertainty of L_{gw}, which can be affected by the stability of the water and the algorithm of the data process. We fast performed five measurements; the stability of the measurement of L_{gw} is 1.3 μm (standard deviation). The second term can be calculated to 1.8×10^{-5}. The third term of Equation (3) is related to the uncertainty of L_a, and the short-term stability of L_a is 0.6 μm (standard deviation). This part can be estimated to be 1.2×10^{-5}. The expansion coefficient is $5 \times 10^{-7}/°C$. The temperature change is about 3.5 °C (from 14.4 °C to 17.9 °C) in long-term experiments. Thermal expansion can be calculated at 0.1 μm, corresponding to 1.8×10^{-6} uncertainty. Finally, the combined uncertainty can be calculated to be 2.2×10^{-5}, with a coverage factor of k=1, which shows a good agreement with the results in Figure 6b.

Based on Equation (2), the measurement uncertainty of n_p is related to L_p, L_a and n_a, and can be calculated as:

$$u_{n_p}{}^2 = \left(\frac{L_p}{L_a} u_{n_a} \right)^2 + \left(\frac{n_a}{L_a} u_{L_p} \right)^2 + \left(\frac{n_p}{L_a} u_{L_a} \right)^2 \tag{4}$$

As mentioned above, the first term of Equation (4) can be neglected. Considering the second term, the short-term stability of L_p is 0.45 μm, corresponding to 0.64×10^{-5} uncertainty of the refractive index. The third term of Equation (4) can be calculated to 1.1×10^{-5} uncertainty. The uncertainty due to thermal expansion is also 1.8×10^{-6}. Therefore, combined uncertainty can be evaluated to be 1.3×10^{-5}, with a coverage factor of $k = 1$, which shows a good agreement with the results in Figure 9b.

5. Conclusions

In this work, we present a method which enables the absolute measurement of the refractive index of water using a frequency comb. Based on changes of the optical path in air and water, the refractive index of water can be determined with high precision, which is of fundamental importance in the

optical method when used underwater. Our results show a measurement uncertainty of 10^{-5}, that is to say, the corresponding measurement uncertainty is only several mm when we measure a distance of up to 100 m underwater. This kind of performance can satisfy most applications. Thanks to the low power attenuation of blue-green light underwater, frequency-comb instruments show great promise for marine technology, significantly improving upon the current technologies. However, the entire system is relatively expensive on account of the cost of the frequency comb. The development of a portable and low-cost frequency comb would solve this problem [43,44].

Author Contributions: Zhaopeng Meng, Xiaoyu Zhai, and Hanzhong Wu proposed the method; Zhaopeng Meng, Xiaoyu Zhai, Zhiyang Wang and Hanzhong Wu designed and performed the experiments; Xiaoyu Zhai, Jianguo Wei and Zhiyang Wang analyzed the data; Zhaopeng Meng, Xiaoyu Zhai and Hanzhong Wu wrote the paper.

Conflicts of Interest: The authors declare no conflict of interest.

References

1. Xu, J.; Kong, M.; Lin, A.; Song, Y.; Han, J.; Xu, Z.; Xu, B.; Gao, S.; Deng, N. Directly modulated green-light diode-pumped solid-state laser for underwater wireless optical communication. *Opt. Lett.* **2017**, *42*, 1664–1667. [CrossRef] [PubMed]

2. Amiri-Simkooei, A.; Snellen, M.; Simons, D. Principal component analysis of single-beam echo-sounder signal features for seafloor classification. *IEEE J. Ocean. Eng.* **2011**, *36*, 259–272. [CrossRef]

3. Petillot, Y.; Tena Ruiz, I.; Lane, D. Underwater vehicle obstacle avoidance and path planning using a multi-beam forward looking sonar. *IEEE J. Ocean. Eng.* **2001**, *26*, 240–251. [CrossRef]

4. Hasan, R.; Ierodiaconou, D.; Monk, J. Evaluation of four supervised learning methods for benthic habitat mapping using backscatter from multi-beam sonar. *Remote Sens.* **2012**, *4*, 3427–3443. [CrossRef]

5. Park, D.; Kwak, K.; Chung, W.; Kim, J. Development of underwater short-range sensor using electromagnetic wave attenuation. *IEEE J. Ocean. Eng.* **2016**, *41*, 318–325.

6. Al-Shamma, A.; Shaw, A.; Saman, S. Propagation of electromagnetic waves at MHz frequencies through seawater. *IEEE Trans. Antennas Propag.* **2004**, *52*, 2843–2849. [CrossRef]

7. Huang, B.; Liu, T.; Hu, H.; Han, J.; Yu, M. Underwater image recovery considering polarization effects of objects. *Opt. Express* **2016**, *24*, 9826–9838. [CrossRef] [PubMed]

8. Gu, Y.; Carrizo, C.; Gilerson, A.; Brady, P.; Cummings, M.; Twardowski, M.; Sullivan, J.; Ibrahim, A.; Kattawar, G. Polarimetric imaging and retrieval of target polarization characteristics in underwater environment. *Opt. Express* **2016**, *55*, 626–637. [CrossRef] [PubMed]

9. Guo, Y.; Song, H.; Liu, H.; Wei, H.; Yang, P.; Zhan, S.; Wang, H.; Huang, H.; Liao, N.; Mu, Q.; et al. Model-based restoration of underwater spectral images captured with narrowband filters. *Opt. Express* **2016**, *24*, 13101–13120. [CrossRef] [PubMed]

10. Bartolini, L.; Dominicis, L.; Collibus, M.; Fornetti, G.; Guarneri, M.; Paglia, E.; Poggi, C.; Ricci, R. Underwater three-dimensional imaging with an amplitude-modulated laser radar at a 405 nm wavelength. *Appl. Opt.* **2005**, *44*, 7130–7135. [CrossRef]

11. Singh, S. Refractive index measurement and its applications. *Phys. Scr.* **2002**, *65*, 167–180. [CrossRef]

12. Schiebener, P.; Straub, J. Refractive index of water and steam as function of wavelength, temperature and density. *J. Phys. Chem. Ref. Data* **1990**, *19*, 677–717. [CrossRef]

13. Harvey, A.; Gallagher, J.; Sengers, J.L. Revised formulation for the refractive index of water and steam as a function of wavelength, temperature and density. *J. Phys. Chem. Ref. Data* **1998**, *27*, 761–774. [CrossRef]

14. Kuhler, K.; Dereniak, E.; Buchanan, M. Measurement of the index of refraction of the plastic Phenoxy PKFE. *Appl. Opt.* **1991**, *30*, 1711–1714. [CrossRef] [PubMed]

15. Moreels, E.; de Greef, C.; Finsy, R. Laser light refractometer. *Appl. Opt.* **1984**, *23*, 3010–3013. [CrossRef] [PubMed]

16. Santic, B.; Gracin, D.; Juraic, K. Measurement method for the refractive index of thick solid and liquid layers. *Appl. Opt.* **2009**, *48*, 4430–4436. [CrossRef] [PubMed]

17. Nemoto, S. Measurement of the refractive index of liquid using laser beam displacement. *Appl. Opt.* **1992**, *31*, 6690–6694. [CrossRef] [PubMed]

18. Lu, W.; Worek, W. Two-wavelength interferometric technique for measuring the refractive index of salt-water solutions. *Appl. Opt.* **1993**, *32*, 3992–4002. [CrossRef] [PubMed]

19. Dobbins, H.; Peck, E. Change of refractive index of water as a function of temperature. *J. Opt. Soc. Am.* **1973**, *63*, 318–320. [CrossRef]

20. Carroll, L.; Henry, M. Autocompensating interferometer for measuring the changes in refractive index of supercooled water as a function of temperature at 632.8 nm. *Appl. Opt.* **2002**, *41*, 1330–1336. [CrossRef] [PubMed]

21. St-Arnaud, J.; Ge, J.; Orbriot, J.; Bose, T.; Marteau, P. An accurate method for refractive index measurements of liquids using two Michelson laser interferometers. *Rev. Sci. Instrum.* **1991**, *62*, 1411–1415. [CrossRef]

22. Richerzhagen, B. Interferometer for measuring the absolute refractive index of liquid water as a function of temperature at 1.064 μm. *Appl. Opt.* **1996**, *35*, 1650–1653. [CrossRef] [PubMed]

23. Harvey, A. Determination of the optical constants of thin films in the visible by static dispersive Fourier transform spectroscopy. *Rev. Sci. Instrum.* **1998**, *69*, 3649–3658. [CrossRef]

24. Kim, C.; Su, C. Measurement of the refractive index of liquids at 1.3 and 1.5 micron using a fiber optic Fresnel ratio meter. *Meas. Sci. Technol.* **2004**, *15*, 1683–1686. [CrossRef]

25. Newbury, N.R. Searching for applications with a fine-tooth comb. *Nat. Photonics* **2011**, *5*, 186–188. [CrossRef]

26. Nishiyama, A.; Yoshida, S.; Hariki, T.; Nakajima, Y.; Minoshima, K. Sensitivity improvement of dual-comb spectroscopy using mode-filtering technique. *Opt. Express* **2017**, *25*, 31730–31738. [CrossRef] [PubMed]

27. Deschenes, J.; Sinclair, L.; Giorgetta, F.; Swann, W.; Baumann, E.; Bergeron, H.; Cermak, M.; Coddington, I.; Newbury, N. Synchronization of distant optical clocks at the femtosecond level. *Phys. Rev. X* **2016**, *6*, 021016. [CrossRef]

28. Balling, P.; Křen, P.; Mašika, P.; van den Berg, S.A. Femtosecond frequency comb based distance measurement in air. *Opt. Express* **2009**, *17*, 9300–9313. [CrossRef] [PubMed]

29. Jin, J.; Kim, J.W.; Kang, C.; Kim, J.; Eom, T.B. Thickness and refractive index measurement of a silicon wafer based on an optical comb. *Opt. Express* **2010**, *18*, 18339–18346. [CrossRef] [PubMed]

30. Mahjoubfar, A.; Goda, K.; Ayazi, A.; Fard, A.; Kim, S.; Jalali, B. High-speed nanometer-resolved imaging vibrometer and velocimeter. *Appl. Phys. Lett.* **2011**, *98*, 101107. [CrossRef]

31. Choi, S.; Yamamoto, M.; Moteki, D.; Shioda, T.; Tanaka, Y.; Kurokawa, T. Frequency-comb-based interferometer for profilometry and tomography. *Opt. Lett.* **2006**, *31*, 1976–1978. [CrossRef] [PubMed]

32. Zhang, J.; Lu, Z.H.; Wang, L.J. Precision measurement of the refractive index of air with frequency combs. *Opt. Lett.* **2005**, *30*, 3314–3316. [CrossRef] [PubMed]

33. Minoshima, K.; Arai, K.; Inaba, H. High-accuracy self-correction of refractive index of air using two-color interferometry of optical frequency combs. *Opt. Express* **2011**, *19*, 26095–26105. [CrossRef] [PubMed]

34. Maeng, S.; Park, J.; Byungsun, O.; Jin, J. Uncertainty improvement of geometrical thickness and refractive index measurement of a silicon wafer using a femtosecond pulse laser. *Opt. Express* **2012**, *20*, 12184–12190. [CrossRef] [PubMed]

35. Kim, J.; Kim, J.; Eom, T.; Jin, J.; Kang, C. Vibration-insensitive measurement of thickness variation of glass panels using double-slit interferometry. *Opt. Express* **2014**, *22*, 6486–6494. [CrossRef] [PubMed]

36. Park, J.; Bae, J.; Jin, J.; Kim, J.; Kim, J. Vibration-insensitive measurements of the thickness profile of large glass panels. *Opt. Express* **2015**, *23*, 32941–32949. [CrossRef] [PubMed]

37. Ciddor, P.E. Refractive index of air: New equations for the visible and near infrared. *Appl. Opt.* **1996**, *35*, 1566–1573. [CrossRef] [PubMed]

38. Van den Berg, S.A.; van Eldik, S.; Bhattacharya, N. Mode-resolved frequency comb interferometry for high-accuracy long distance measurement. *Sci. Rep.* **2015**, *5*, 14661. [CrossRef] [PubMed]

39. Zhu, Z.; Xu, G.; Ni, K.; Zhou, Q.; Wu, G. Synthetic-wavelength-based dual-comb interferometry for fast and precise absolute distance measurement. *Opt. Express* **2018**, *26*, 5747–5757. [CrossRef] [PubMed]

40. Vaughan, R.; Scott, N.; White, D. The theory of bandpass sampling. *IEEE Trans. Signal Proc.* **1991**, *39*, 1973–1984. [CrossRef]

41. Groot, P.; Deck, L. Three-dimensional imaging by sub-Nyquist sampling of white-light interferograms. *Opt. Lett.* **1993**, *18*, 1462–1464. [CrossRef] [PubMed]

42. Wu, G.; Zhou, Q.; Shen, L.; Ni, K.; Zeng, X.; Li, Y. Experimental optimization of the repetition rate difference in dual-comb ranging system. *Appl. Phys. Express* **2014**, *7*, 106602. [CrossRef]

43. Lee, C.; Chu, S.; Little, B.E.; Bland-Hawthorn, J.; Leon-Saval, S. Portable frequency combs for optical frequency metrology. *Opt. Express* **2012**, *20*, 16671–16676. [CrossRef]

44. Wu, H.; Zhao, T.; Wang, Z.; Zhang, K.; Xue, B.; Li, J.; He, M.; Qu, X. Long distance measurement up to 1.2 km by electro-optic dual-comb interferometry. *Appl. Phys. Lett.* **2017**, *111*, 251901. [CrossRef]